

Effects of ^4He film on quartz tuning forks in ^3He at ultra-low temperatures

T. S. Riekkı · J. Rysti · J. T. Mäkinen ·
A. P. Sebedash · V. B. Eltsov ·
J. T. Tuoriniemi

Received: date / Accepted: date

Abstract In pure superfluid $^3\text{He-B}$ at ultra-low temperatures, quartz tuning fork oscillator response is expected to saturate when the dissipation caused by the superfluid medium becomes substantially smaller than the internal dissipation of the oscillator. However, even with small amount of ^4He covering the surfaces, we have observed saturation already at significantly higher temperatures than anticipated, where we have other indicators to prove that the ^3He liquid is still cooling. We found that this anomalous behavior has a rather strong pressure dependence, and it practically disappears above the crystallization pressure of ^4He . We also observed a maximum in the fork resonance frequency at temperatures where the transition in quasiparticle flow from the hydrodynamic to the ballistic regime is expected. We suggest that such anomalous features derive from the superfluid ^4He film on the oscillator surface.

Keywords Quartz tuning fork · Helium-3 · Helium-3–Helium-4 mixture · Helium-4 film

T. S. Riekkı[†] · J. Rysti · J. T. Mäkinen · V. B. Eltsov · J. T. Tuoriniemi
Aalto University - School of Science
Department of Applied Physics
Low Temperature Laboratory
P.O. BOX 15100 FI-00076 Aalto, Finland
[†]E-mail: tapio.riekki@aalto.fi
A. P. Sebedash
P. L. Kapitza Institute for Physical Problems RAS
Kosygina 2, 119334 Moscow, Russia

1 Introduction

Quartz tuning forks (QTFs) are used for temperature, pressure, viscosity and turbulence measurements in normal and superfluid helium [1, 2, 3, 4]. These influence the width (full width at half maximum) and the frequency of the fork resonance. The characteristic dimensions of a typical QTF may also match the wavelength of first or second sound in pure helium or isotope mixtures, at certain temperature and pressure, resulting in acoustic phenomena [5, 6, 7] that are interesting in their own right, but can also make interpreting the fork data more difficult.

On cooling of ^3He below the superfluid transition temperature T_c , the dissipation caused by thermal excitations, or quasiparticles, becomes smaller, as their number decreases, which is observed as reduction in the QTF resonance width. In the B-phase at the lowest temperatures, the quasiparticle density decreases exponentially with temperature, and eventually dissipation caused by the quasiparticles becomes smaller than the internal dissipation of the fork, giving typically a residual width 10-20 mHz, which poses the low-temperature limit for thermometry.

When ^4He is added to a ^3He system, the fork analysis becomes more complex, as the surfaces become coated with ^4He [8, 9]. Below 100 mK, the ^4He layer becomes superfluid [10], and due to superfluid film flow it will spread out to cover all the surfaces of the experimental cell. The film will change the quasiparticle reflection conditions [11] on the QTF surface affecting its resonance response. At sufficiently high pressures, the ^4He layer becomes solid, and is no longer mobile as a liquid layer would be. However, even the presence of solid layer may affect the quasiparticle reflection conditions, provided that the layer is thick enough to affect the surface roughness.

Boldarev *et al.* [12] observed in the ^3He -rich phase of phase-separated ^3He - ^4He mixture, between 15 and 350 mK, that the QTF deviated from the predicted viscosity and density dependent response. They attributed this anomalous behavior to the ^4He film covering the surface of the QTF, which they estimated to have thickness of several microns. The non-trivial response made the fork calibration more difficult, but in their experiment the fork still had clear temperature sensitivity.

We have studied the behavior of ^4He -coated quartz tuning forks in ^3He at temperatures below 1 mK, where we observed saturation in the QTFs' response at higher temperatures than anticipated. We have two independent experiments that demonstrate similar saturation behavior: one is a nafen-filled ^3He cell with surfaces coated with approximately 3 atomic layers of ^4He , and the other an adiabatic melting cell that contains saturated ^3He - ^4He mixture at ^4He crystallization pressure, where we expect a much thicker equilibrium film. In both experiments we have also observed a maximum in the resonance frequency at temperatures where the quasiparticle flow regime changes from the hydrodynamic to the ballistic one. In this paper we focus on reporting our experimental observations, while the detailed explanation on the origin of the effects remains a task for the future.

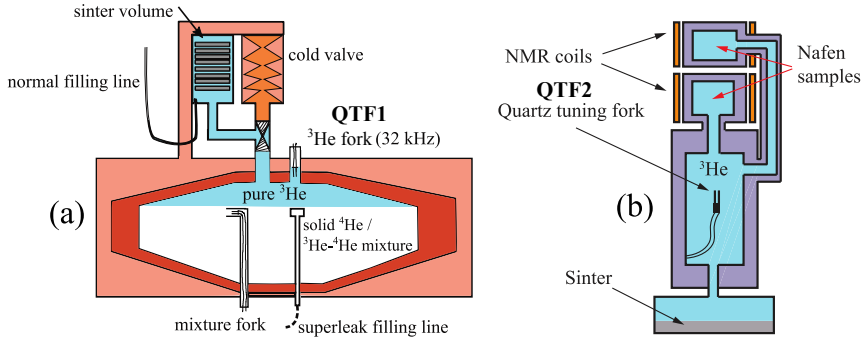


Fig. 1 (color online) Schematic drawings of the experimental cells. The adiabatic melting cell (a) consists of a large main volume and a sinter-filled heat exchanger volume separated by a cold valve. The cell is monitored with two quartz tuning fork oscillators, one in the ^3He phase (QTF1) and another in the mixture phase (or frozen in solid ^4He , depending on the stage of the experimental run). The nafen cell (b) has two separate samples with different nafen densities. They are both connected to a volume of bulk ^3He , where the thermometer quartz tuning fork (QTF2) is located. The cell is mounted on the nuclear stage of a rotating cryostat. The surfaces in both systems are coated with a layer of ^4He , although of different thickness.

2 Results

2.1 ^3He in phase-separated ^3He - ^4He mixture at ^4He crystallization pressure

In the adiabatic melting experiment [13,14,15], sub-0.1 mK temperatures in ^3He - ^4He mixtures are pursued at ^4He crystallization pressure 25.64 bar [16, 17] by first precooling a system of solid ^4He and liquid ^3He with an adiabatic nuclear refrigerator, and then allowing the solid to melt by extracting ^4He , mixing the two isotopes providing cooling [18].

Fig. 1a shows a sketch of the melting experiment cell. More details of this setup can be found in Ref. [19]. The resonance width of the QTF in mixture is about 400 Hz, and the effects of the ^4He coating on its behavior are indistinguishable. On the other hand, the resonance width of the QTF in ^3He (QTF1), located at the top of the main cell volume, reaches approximately 0.2 Hz at the end of the melting process, and then the superfluid ^4He film causes it to have an anomalous response.

Fig. 2 shows the QTF1 response during the melting process. The fork was measured in the tracking mode which enables us to receive datapoints every few seconds even at very narrow widths by assuming a Lorentzian lineshape with a constant area [2]. The melting was started at around 4 Hz resonance width, corresponding to about $0.19T_c \approx 0.5\text{ mK}$ temperature. Initially the resonance width decreases rapidly as the cell cools down, and the narrowest widths are already reached within the first few minutes of the process. The temperature calibration for the QTF1 was obtained using the self-calibration method described in Ref. [20]. The observed 150 mHz resonance width would then correspond to about $0.11T_c \approx 0.3\text{ mK}$. At this temperature with the ^4He

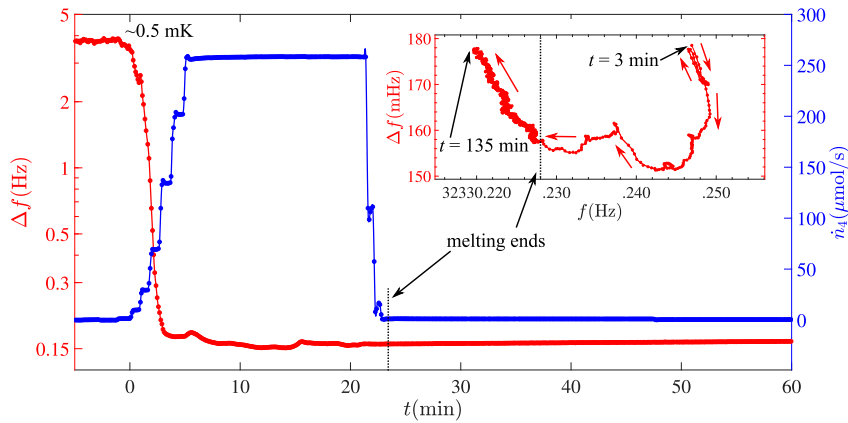


Fig. 2 (color online) (Main panel) Left y-axis: resonance width of the quartz tuning fork (QTF1) in the ^3He phase during the melting process with zero time chosen to be at the beginning of the melting. Right y-axis: ^4He extraction rate. (Inset) QTF1 resonance width versus resonance frequency during the coldest stage of the run, showing the saturation of the width value, and the anomalous features that occur during the melting. Red arrows indicate the direction of time; at around 3 min the width backtracks slightly and then continues to decrease.

extraction rate $\dot{n}_4 \approx 260 \mu\text{mol/s}$, the cooling power of the melting process [18] is approximately 2 nW. This is a much larger value than the heat leak to the cell 0.1 nW, which was estimated during the warm-up period, after the melting, when the QTF1 width started to have temperature sensitivity again. Also, the viscous heating effects during the melting are considered insignificant. With the estimated heat leak, the liquid should cool down to below 0.3 mK, suggesting that the resonance width is no longer proportional to the quasiparticle density in bulk. Even after the melting was stopped, the QTF1 did not show any rapid change from the saturation value which indicates that the actual temperature of the liquid was lower than the value given by the resonance width. The fork's self-calibration relies on the transition to the ballistic flow regime, the point of which cannot be determined precisely. However, we do not believe that the uncertainty in the temperature calibration could explain the discrepancy between the temperature given by the QTF1 and the cooling power of the melting process. Even at 0.1 mK, with $260 \mu\text{mol/s}$ ^4He extraction rate, the cooling power 0.2 nW is still larger than the estimated external heat leak.

The inset in Fig. 2 shows that during the melting, there appears anomalous features on the QTF1's frequency-width plot. These resonance-like features only occur while the melting is being carried out; they do not reproduce when the cell is slowly warming up after the melting is over. We point out that during the melting period the distance between the fork and the ^3He -mixture phase-separation boundary is changing. As the melting is being carried out, ^3He is dissolved into ^4He released from the solid, decreasing the volume of the ^3He phase, while increasing the volume of the mixture phase. When the

mixture phase, containing ^4He , approaches QTF1, it will increase the thickness of the ^4He film covering the fork due to the Rollin film effect [21,22]. Another observation, that seems to corroborate the phase-separation boundary vicinity effect, is the 30 mHz resonance frequency shift from the before-melting value that remained even after the melting had been stopped.

2.2 ^3He with small amount of ^4He present

The nafen experiment consists of two separate samples of ^3He confined in the nematic nano-material nafen [23], which are connected to a volume of bulk ^3He (Fig. 1b). The temperature of helium is controlled by changing the magnetic field applied to the nuclear demagnetization cooling stage. The properties of ^3He in the two nafen samples are probed by means of nuclear magnetic resonance (NMR). A quartz tuning fork in the bulk ^3He volume (QTF2) is used as a thermometer. In this experiment ^4He is present only to coat the surfaces of nafen to prevent the formation of paramagnetic solid ^3He [24]. The thickness of ^4He on the nafen strands was determined to be approximately 2.5 atomic layers [24]. The surfaces, including the quartz tuning fork, could adsorb more ^4He , thus the ^4He layer was not maximal [24]. This was clearly demonstrated after the measurements presented in this paper, as adding more ^4He into the system and repressurizing back to 29.5 bar changed the tuning fork width at the bulk ^3He superfluid transition from 800 Hz to 570 Hz.

Fig. 3a shows the QTF2 resonance width and the NMR frequency shift during cooling and warming of the sample at 3 bar pressure. These two quantities give independent measurements of temperature. The tuning fork width displays a resonance-like feature at 1.1 A current in the demagnetization magnet, a minimum of about 4 Hz at 0.9 A, and an eventual saturation to 9 Hz toward the lowest temperatures. The NMR frequency shift, on the other hand, indicates continuous cooling of the sample all the way down to the lowest demagnetization current. The NMR frequency of superfluid ^3He , in the polar phase confined in nafen, is shifted from the Larmor value as a function of temperature in axial magnetic field [25]. The QTF2 was measured by continuously sweeping over the resonance.

Fig. 4 plots the QTF2 resonance width and frequency at 23 bar during slow cooling and warming. Here the QTF2 was measured by applying pulse excitation and recording the ring-down signal. This gives superior data acquisition rate and noise at small resonance widths compared to the continuous sweeping method. Multiple resonance-like features are seen together with a shallow minimum in the width and an eventual saturation to about 1 Hz. In the absence of anomalous behavior, QTF2 width of 1 Hz would correspond to about $0.16T_c$ temperature, or 0.4 mK at 23 bars. The frequency of the oscillator continues to change even after the width has saturated. The same pattern is repeated during warming of the sample, but the QTF2 response does not return exactly along the same path.

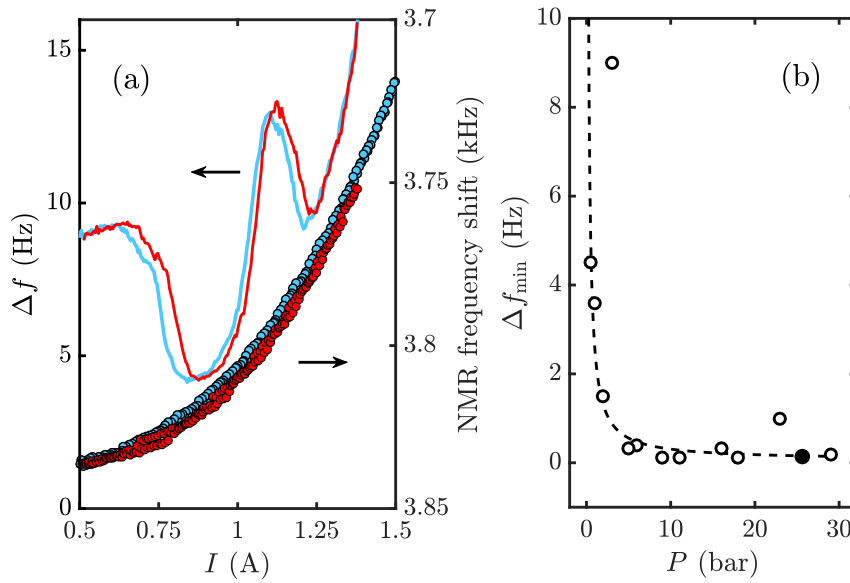


Fig. 3 (color online) (a): Quartz tuning fork width (solid lines) and NMR frequency shift (dots) from the Larmor frequency (363 kHz) at 3 bar pressure as functions of the demagnetization magnet current, which controls the temperature of the sample. Blue color indicates cooling and red warming. (b): Narrowest QTF widths as a function of pressure. The dashed curve is a guide to the eye. Open points are from the nafen experiment and the black point from the adiabatic melting experiment.

The anomalous behavior of the tuning fork strongly depends on pressure. It is present at 23 bars, where resonance-like features are observed and the tuning fork width would not go below 1 Hz. At 29 bar pressure, which is above the crystallization pressure of ^4He , there is no indication of any anomalies and the tuning fork width could be reduced to 190 mHz without evidence of saturation (inset of Fig. 4). Measurements have been performed at various pressures, but the QTF2 was measured using the pulse method only at 23 and 29 bars. The continuous sweeping method may not reveal small anomaly patterns of the oscillator or the saturation. At 3 bar pressure the anomaly is the strongest. The minimum attained resonance widths as a function of pressure are plotted in Fig. 3b. Small resonance-like features are visible at 16, 6, 5, and 2 bar pressures, even with the sweeping QTF2 measurement.

The resonance-like features could be attributed to the first sound resonances in the tuning fork cavity [26]. The diameter of our tuning fork volume (9 mm) and the oscillator frequency (32 kHz) match roughly the frequencies of radial acoustic modes, especially at lower pressures, where the speed of first sound is smaller. It is not clear without more detailed analysis if the resonance-like features seen at 23 bar can be explained by acoustic resonances. The absence of these anomalies at 29 bar pressure might be due to the larger speed of sound.

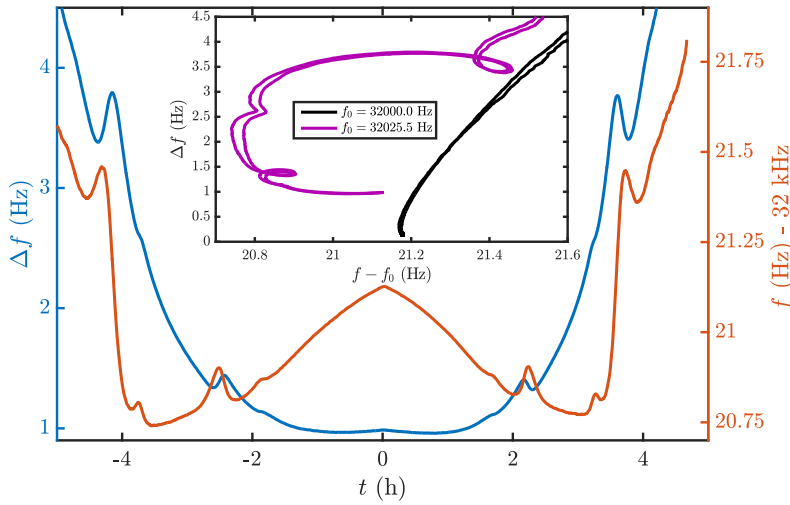


Fig. 4 (color online) Quartz tuning fork width and frequency at 23 bar during cooling ($t < 0$) and warming ($t > 0$) of the nafen cell over a 10-hour period, demonstrating multiple resonance modes and saturation of the tuning fork width. A minimum of the width is reached at approximately ± 0.7 h. The inset plots the QTF width in terms of frequency at 23 bar (red) and at 29 bar (black).

2.3 QTF resonance frequency maximum

In both the used setups, we have also observed a resonance frequency maximum in the forks' response, at around $0.25T_c$. This is illustrated in the main panel of Fig. 5. The inset additionally shows the case of reduced ^4He amount in the nafen cell. In this case, the maximum disappears, and the resonance frequency instead saturates at the lowest temperatures, which is consistent with observations in pure ^3He [20].

The appearance of the frequency maximum with the increasing ^4He coverage probably originates from the change in ^3He quasiparticle scattering conditions on the QTF surface [11], as the thickness of the film grows. The maximum occurs at around the temperatures, in which the quasiparticle flow is expected to change from the hydrodynamic to the ballistic flow regime, and it could possibly be used as an indicator of such. Thus the maximum could be utilized in the QTF self-calibration described in Ref. [20].

3 Conclusions

We have observed a saturation in the temperature dependence of the resonance width of quartz tuning fork oscillators in two independent experiments in ^3He systems with surfaces coated by ^4He . In the melting experiment, the

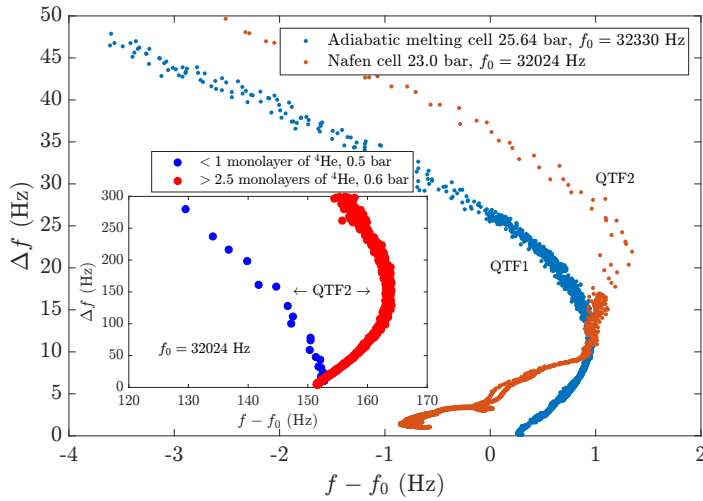


Fig. 5 (color online) Main panel: Fork resonance width as a function of the resonance frequency in the adiabatic melting experiment (blue, QTF1) and in the nafen experiment (orange, QTF2), both of which show a maximum in the resonance frequency. The resonance frequencies have been shifted by f_0 , given in the legend. The inset shows that the maximum disappears if the ^4He content of the cell is low enough.

temperature indicated by the QTF resonance width saturates to a value at which the cooling power of the helium isotope mixing process would still be significantly larger than the external heat leak. In the nafen experiment, on the other hand, we had an NMR-based thermometry that showed further cooling in the experimental cell, even after the QTF width had saturated. We also observed strong pressure dependence in the value of the saturated width, with the maximum being at 3 bar. Both setups also displayed a maximum in the QTF resonance frequency, which appears only if there is enough ^4He in the system.

We suggest that this behavior originates from the ^4He film covering the QTF, however, the detailed understanding of the phenomenon requires more work. In particular, studying the dependence on the fork size might be important. As a practical conclusion, forks covered by ^4He remain relatively reliable thermometers only down to widths of about 1 Hz, provided that the geometry of the fork volume excludes coupling to the acoustic modes. At pressures near the ^4He crystallization pressure, this limit corresponds to approximately $0.16T_c$.

Acknowledgements This work was supported in part by the Jenny and Antti Wihuri Foundation (Grant No. 00170320), and it utilized the facilities provided by Aalto University at OtaNano - Low Temperature Laboratory infrastructure. We also acknowledge the support by the European Research Council (ERC) under the European Union’s Horizon 2020 research and innovation programme (Grant Agreement No. 694248).

References

1. R. Blaauwgeers, M. Blazkova, M. Človečko, V. B. Eltsov, R. de Graaf, J. Hosio, M. Krusius, D. Schmoranzler, W. Schoepe, L. Skrbek, P. Skyba, R. E. Solntsev, D. E. Zmeev, *J. Low Temp. Phys.* **146**, 537 (2007). DOI 10.1007/s10909-006-9279-4
2. E. Pentti, J. Rysti, A. Salmela, A. Sebedash, J. Tuoriniemi, *J. Low Temp. Phys.* **165**, 132 (2011). DOI 10.1007/s10909-011-0394-5
3. D. I. Bradley, M. J. Fear, S. N. Fisher, A. M. Guénault, R. P. Haley, C. R. Lawson, P. V. E. McClintock, G. R. Pickett, R. Schanen, V. Tsepelin, L. A. Wheatland, *J. Low Temp. Phys.* **156**, 116 (2009). DOI 10.1007/s10909-009-9901-3
4. J. T. Mäkinen, V. B. Eltsov, *Phys. Rev. B* **97**, 014527 (2018). DOI 10.1103/PhysRevB.97.014527
5. J. Rysti, J. Tuoriniemi, *J. Low Temp. Phys.* **177**, 133 (2014). DOI 10.1007/s10909-014-1203-8
6. T. S. Riekkii, M. S. Manninen, J. T. Tuoriniemi, *Phys. Rev. B* **94** 224514 (2016). DOI 10.1103/physrevb.94.224514
7. A. Salmela, J. Tuoriniemi, J. Rysti, *J. Low Temp. Phys.* **162**, 678 (2010). DOI 10.1007/s10909-010-0246-8
8. V. P. Peshkov, *JETP Lett.* **21**, 162-164 (1975). DOI 10.1103/physrevb.39.8934
9. S. Murakawa, M. Wasai, K. Akiyama, Y. Wada, Y. Tamura, R. Nomura, Y. Okuda, *Phys. Rev. Lett.* **108** 025302 (2012). DOI 10.1103/PhysRevLett.108.025302
10. G. Agnolet, D. F. McQueeney, J. D. Reppy, *Phys. Rev. B* **39**, 8934 (1989). DOI 10.1103/physrevb.39.8934
11. D. Kim, M. Nakagawa, O. Ishikawa, T. Hata, T. Kodama, *Phys. Rev. Lett.* **71**, 1581-1584 (1993). DOI 10.1103/PhysRevLett.71.1581
12. S. T. Boldarev, R. B. Gusev, S. I. Danilin, A. Y. Parshin, *Instrum. Exp. Tech.* **54**, 740 (2011). DOI 10.1134/s0020441211050101
13. A. P. Sebedash, *JETP Lett.* **65**, 276 (1997). DOI 10.1134/1.567360
14. A. P. Sebedash, J. T. Tuoriniemi, S. T. Boldarev, E. M. M. Pentti, A. J. Salmela, *J. Low Temp. Phys.* **148**, 725 (2007). DOI 10.1007/s10909-007-9443-5
15. J. Tuoriniemi, J. Martikainen, E. Pentti, A. Sebedash, S. Boldarev, G. Pickett, *J. Low Temp. Phys.* **129**, 531 (2002). DOI 10.1023/a:1021468614550
16. E. Pentti, J. Tuoriniemi, A. Salmela, A. Sebedash, *J. Low Temp. Phys.* **146**, 71-83 (2006). DOI 10.1007/s10909-006-9267-8
17. A. Salmela, A. Sebedash, J. Rysti, E. Pentti, J. Tuoriniemi, *Phys. Rev. B* **83** 134510 (2011). DOI 10.1103/physrevb.83.134510
18. T. S. Riekkii, A. P. Sebedash, J. T. Tuoriniemi, arXiv:1810.10432 (2018)
19. A. Sebedash, S. Boldarev, T. Riekkii, J. Tuoriniemi, *J. Low Temp. Phys.* **187**, 588 (2017). DOI 10.1007/s10909-017-1755-5
20. I. Todoshchenko, J. P. Kaikkonen, R. Blaauwgeers, P. J. Hakonen, A. Savin, *Rev. Sci. Instrum.* **85**, 085106 (2014). DOI 10.1063/1.4891619
21. B. V. Rollin, F. Simon, *Physica* **6** 219-230 (1939). DOI 10.1016/S0031-8914(39)80013-1
22. H. A. Fairbank, C. T. Lane, *Phys. Rev.* **76**, 1209-1211 (1949). DOI 10.1103/PhysRev.76.1209
23. V. E. Asadchikov, R. S. Askhadullin, V. V. Volkov, V. V. Dmitriev, N. K. Kitaeva, P. N. Martynov, A. A. Osipov, A. A. Senin, A. A. Soldatov, D. I. Chekrygina, A. N. Yudin, *JETP Lett.* **101**, 556 (2015). DOI 10.1134/S0021364015080020
24. V. V. Dmitriev, A. A. Soldatov, A. N. Yudin, *Phys. Rev. Lett.* **120**, 075301 (2018). DOI 10.1103/PhysRevLett.120.075301
25. S. Autti, V. V. Dmitriev, J. T. Mäkinen, A. A. Soldatov, G. E. Volovik, A. N. Yudin, V. V. Zavjalov, V. B. Eltsov, *Phys. Rev. Lett.* **117**, 255301 (2016). DOI 10.1103/PhysRevLett.117.255301
26. J. T. Tuoriniemi, M. S. Manninen, J. Rysti, *J. Phys. Conf. Ser.* **568**, 012023 (2014). DOI 10.1088/1742-6596/568/1/012023